BROOKHAVEN NATIONAL LABORATORY

BNL--46862

DE92 005038

November, 1991

Hadron Spectroscopy and B Physics at RHIC

S. U. Chung, D. P. Weygand and H. J. Willutzki

Physics Department, Brookhaven National Laboratory,Upton, NY 11973. U.S.A.

ABSTRACT

A description is given of the physics opportunities at RHIC regarding quark-gluon spectroscopy. The basic idea is to isolate with appropriate triggers the sub-processes pomeron + pomeron $\rightarrow$ hadrons and $\gamma^* + \gamma^* \rightarrow$ hadrons with the net effective mass of hadrons in the range of 1.0 to 10.0 GeV, in order to study the hadronic states composed of quarks and gluons. The double-pomeron interactions are expected to produce glueballs and hybrids preferentially, while the two-offshell-photon initial states should couple predominantly to quarkonia and multiquark states.

Of particular interest is the possibility of carrying out a CP-violation study in the self-tagging B decays, $B^0_d \rightarrow K^+\pi^-$ and $\bar{B}^0_d \rightarrow K^-\pi^+$.

1. Hadron Physics at RHIC

In this section is described a conceptual design for carrying out a study of quark-gluon spectroscopy at the BNL Relativistic Heavy Ion Collider (RHIC)[1]. The current design is an updated, upgraded version of that presented at the Fourth Workshop[2] on Experiments and Detectors for RHIC, held at BNL in July 1990.

The idea is derived from a double-pomeron exchange trigger which was successfully implemented in R807 (an ISR experiment at CERN)[3]. The resulting $\pi^+\pi^-$ (see Fig. 1) and K^+K^- spectra provided key ingredients in the study of $J^{PC} = 0^{++}$ states[4] with masses around 1.0 GeV.

For the trigger to succeed, it is necessary that for $p \times p$ the recoiling beam particles come off at a very small angle, $\theta \leq 2$ mr. At RHIC energies this corresponds to installing a set of four 'Roman pots,' two on each side up and down, 10 m away from the intersection region. Precision 5x5 cm mini-drift chambers and scintillation counters will be installed in each Roman pot to detect and trigger on the scattered beam particles. The intersection region will be instrumented with a 4π-detector consisting of cylindrical drift chambers, ring-imaging Cerenkov counters and lead-scintillator barrel counters, all within a 7.2m-long solenoid magnet with a 4.1 m coil diameter, patterned after the Mark III[5] and the ARGUS apparatus.

It was shown in R807 that imposition of momentum balance in the direction perpendicular to that of the beam particles results in pure exclusive events, as follows:

$$pp \rightarrow p\left(\pi^+\pi^-\right)p$$
$$pp \rightarrow p\left(K^+K^-\right)p$$

where the systems shown in parentheses indicate the particles detected in the central detector. In the proposed RHIC experiment, the central detector will be optimized for charged as well as neutral particles with momenta up to 3 GeV/c, so that the following

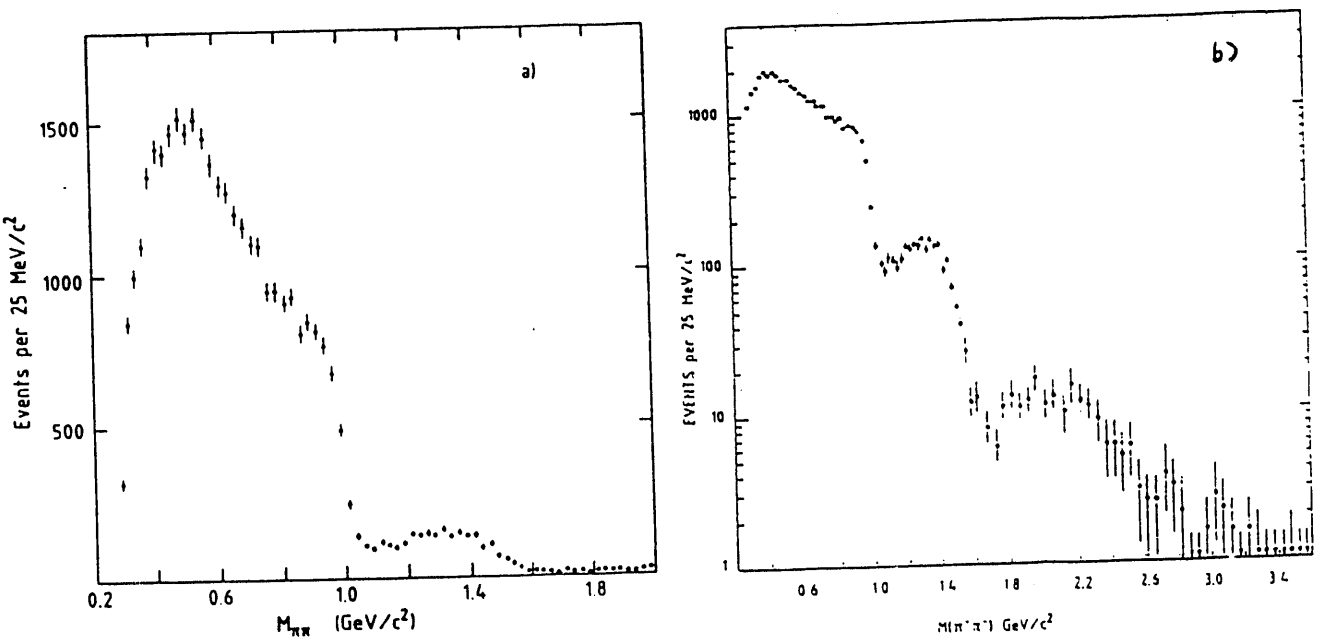

Figure 1: $\pi^+\pi^-$ spectra for $pp \rightarrow p(\pi^+\pi^-)p$ at $\sqrt{s}$ =63 GeV. (a) Raw $M(\pi^+\pi^-)$ spectrum. (b) Acceptance-corrected spectrum on log scale.

reactions can be studied:

$$pp \rightarrow p(\eta\eta)p$$

$$pp \rightarrow p(\omega\omega)p$$

$$pp \rightarrow p(\phi\phi)p$$

$$pp \rightarrow p(\eta\pi\pi)p$$

$$pp \rightarrow p(\omega\pi\pi)p$$

$$pp \rightarrow p(K\bar{K}\pi)p$$

$$pp \rightarrow p(p\bar{p}\pi)p$$

where the parentheses indicate again the central system.

The momentum transfer squared from initial to final protons is given by

$$-t \simeq (p\alpha)^2 \simeq q^2 \simeq 0.25 \text{ (GeV/c)}^2$$

where $p = 250$ GeV/c is the momentum of the initial proton and $\alpha \simeq 2$ mr is the scattering angle of the proton in the laboratory and $q \simeq 0.5$ GeV/c is the momentum of the final proton perpendicular to the beam. Since the slope of $-t$ distributions is expected to be around 10 GeV^{-2} at the top end of RHIC energy[6], the value $-t$ is sufficiently small to guarantee a pomeron exchange, and a double pomeron exchange reaction will result if both the final protons come off with $-t \leq 0.25$ (GeV/c)^2. In this case the central rapidity region corresponds in effect to the reaction

$$\mathbf{PP} \rightarrow \text{hadrons}$$

where **P** stands for a pomeron and the $\sqrt{s}$ for this subprocess ranges from 1.0 to 3.0 GeV. The upper limit on the $\sqrt{s}$ is not an inherent limitation; for a study of the states with $c(b)$ quarks, it should be extended to 5.0(10.0) GeV.

Let M denote the invariant mass of the total hadronic system, i.e. the $\sqrt{s}$ for the process given above. Then,

$$M^2 \simeq \epsilon_1 \epsilon_2 (2p)^2 + t_1 + t_2 - 2\mathbf{q_1} \cdot \mathbf{q_2}$$

where subscripts 1 and 2 denote final deflected beam particles and $1 - \epsilon$ stands for the Feynman x variables[7]. Replacing $-t$ by q^2, one obtains

$$M^2 \simeq \epsilon_1 \epsilon_2 (2p)^2 - (\mathbf{q_1} + \mathbf{q_2})^2$$

From this one sees that

$$\epsilon_1 \sim \epsilon_2 \sim \frac{M}{2p} \simeq 4 \times 10^{-3}$$

for $M = 2$ GeV and $p = 250$ GeV/c.

According to S. Y. Lee (BNL), one can choose an insertion mode in which the angular dispersion of the beam can be held to as low as 1.0 mr at 10 m from the intersection. At this point, the deflected particles may range from 10 mm to 40 mm measured from the beam center. This corresponds to q in the range of 0.25 GeV/c to 1.0 GeV/c for a proton

beam at 250 GeV/c. Within the Roman pots there will be a set of four drift-chamber modules and two scintillation counters, each with an active area measuring 50x50 mm.

The same experimental setup can be applied to heavy-ion collisions, e.g. those involving gold. M. Rhodes-Brown (BNL) points out that in the extreme low-momentum-transfer region the photon-photon interactions become competitive with the double-pomeron production,

$$\sigma \sim (Z\alpha)^4 \sim 0.1$$

for $Au \times Au$ at 100 GeV/u. The heavy ions of RHIC thus provide an opportunity for a study of two offshell-photon interactions,

$$\gamma^*\gamma^* \rightarrow \text{hadrons}$$

where $\sqrt{s}$ for this subprocess is in the range 1.0–3.0 GeV. Note that the photons involved can be highly offshell indeed; the $-t$ corresponding to the photon is given by

$$-t \simeq q^2 < (p \times 1 \text{ mr})^2 \simeq 400 \text{ (GeV/c)}^2$$

where $p = 197 \times 100$ GeV/c and 1 mr is the allowed angular dispersion of the beam.

The coherent production of hadrons by the two-photon process involves extremely sharp $-t$ distributions. According to A. Skuja and D. H. White[8], the slope of the $-t$ distributions is 700 GeV^{-2} for $Au \times Au$ at 100 GeV/u, indicating that the beams simply pass through undeflected in the region where the cross section is appreciable. The energy loss is also extremely small,

$$\epsilon_1 \sim \epsilon_2 \sim \frac{M}{2p} \simeq 5 \times 10^{-5}$$

for $M = 2$ GeV and $p = 197 \times 100$ GeV/c. It is seen that this loss factor is well within the allowed beam dispersion of RHIC.

It therefore follows that a proper $\gamma^*\gamma^*$ trigger calls for something other than the Roman pots, i.e. it has to rely on a veto on the deflected beam, by a set of four lead-scintillation sandwich barrel counters located at 10 m and 40 m away from the intersection point. A barrel counter consists of six truncated wedge detectors with widths 5 cm and 20 cm and 50 cm long. Its design is identical to that of the EM calorimeter in the central detector, as described in the section 3. Note that each barrel counter covers radial distances down to

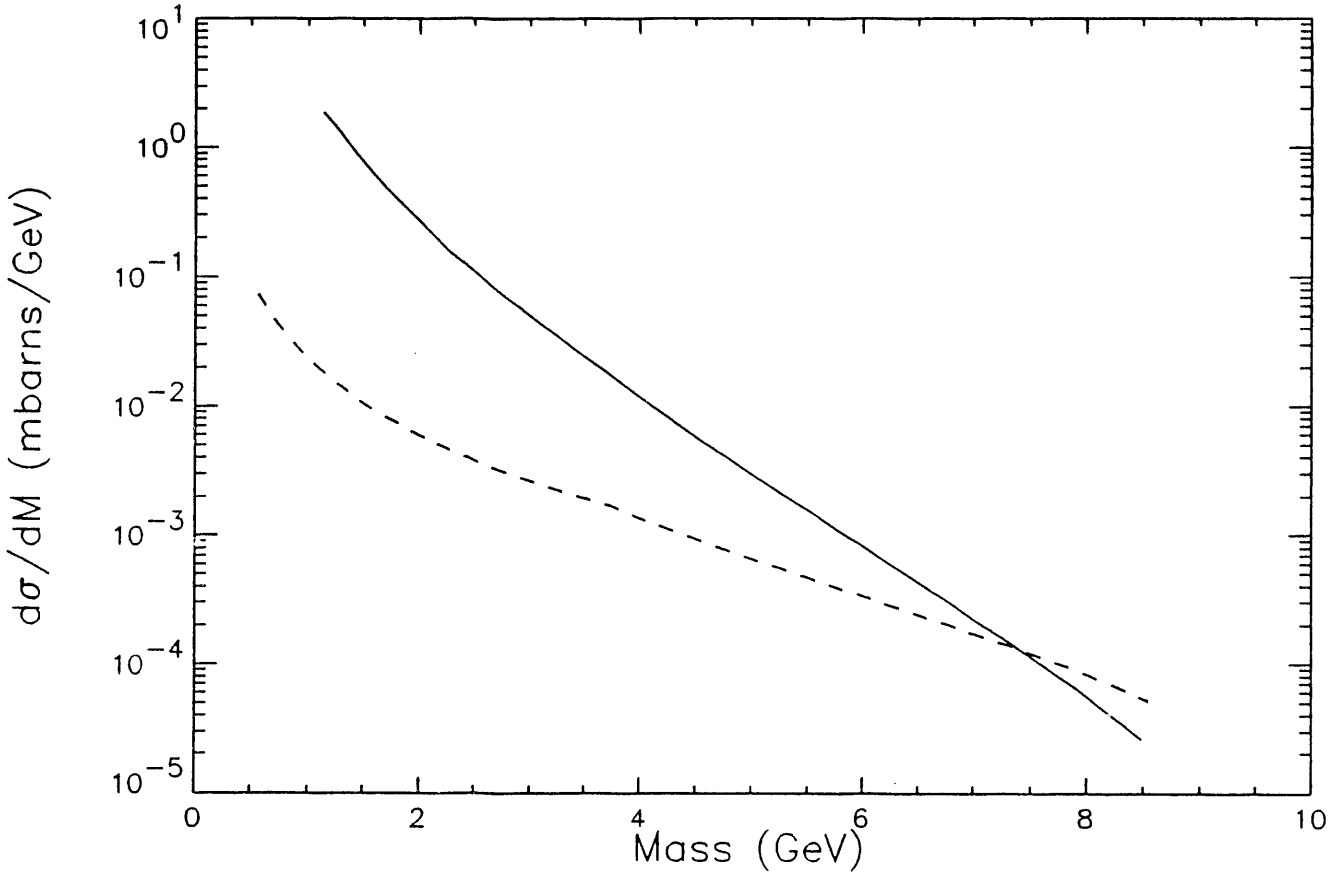

Figure 2: The cross section for two-photon processes as a function of mass M of the central system with its rapidity limited to $|y| < 1$ (the solid curve). The dashed curve corresponds to the same for double-Pomeron processes.

5 cm radius from the beam line. With this setup, one can span the deflection angles from 1.25 mr to 5 mr.

It is necessary, in addition, to veto on the diffractive dissociation of the beam. For this purpose, the end iron-plates of the magnet will be cut out at 100 cm radius, and a hadron calorimeter will be installed, which consists of 30 iron-scintillation sandwiches, designed to veto hadrons above 10 GeV/c. Additional material on the calorimeter is given in the section 3.

The cross sections for production of a central system of mass M through double-Pomeron and two-photon processes have been calculated.[9] Limiting the rapidity of the central system to $|y| < 1$ and the mass M between 1 and 10 GeV, one obtains $\sigma(\mathbf{PP}) \simeq$ 109 μb for $p \times p$ at 100 GeV/c and $\sigma(\gamma\gamma) \simeq 1.11$ mb for $Au \times Au$ at 100 GeV/u. The mass dependence of the cross sections is given in Fig. 2. The double-Pomeron cross section has roughly a M^{-2} dependence, whereas the two-photon cross section drops off much more sharply, even though it is some ten times larger than that of double-Pomeron process for small values of M ($M < 3$ GeV). This shows that two-photon processes are useful mainly for study of hadrons involving light-mass quarks.

What quantum numbers are allowed for the initial state? A Pomeron is not a physical particle, and it should behave as if a continuum of spin states is associated with the exchanged Regge trajectory. According to P. V. Landshoff (private communication), the first physically allowed state on the Pomeron trajectory is the $J^{PC} = 2^{++}$ state which may be the tensor glueball. Assuming a system of two Pomerons to be that of two $J^{PC} = 2^{++}$ particles obeying the Bose-Einstein statistics, one can expect the system (with $I^G = 0^+$) to couple to all possible J^P states with the constraint that C and $L + S$ be even, where L is the orbital angular momentum between the two Pomerons and S is their total intrinsic spin. For the two-photon initial state, one may expect $I^G = 0^+, 1^-$ and $J^{PC} = (0,1,2,3,4,..)^{++}, (0,1,2,3,\ 4,..)^{-+}$. It should be noted that $J^{PC} = (1,3,5,..)^{-+}$, allowed for both double-Pomeron and two-photon initial states, is exotic and cannot couple to quarkonia.

It should be borne in mind that, given the sharp $-t$ distribution in heavy-ion interactions, the photons may in fact behave as if they were on-shell, i.e. zero-mass, especially for hadron effective masses greater than 1.5 GeV. In this case, the allowed values of J^{PC} are more restricted; in particular, the spin-1 states do not couple to two real photons. It may be useful to work this result out in some detail. Consider a decay of a state of spin J and parity η into two identical particles of spin-1 with helicities λ_1 and λ_2; its decay amplitude is given by[10,11]

$$A \propto F^J_{\lambda_1\lambda_2} \left[D^J_{M\lambda}(\phi,\theta,0)\right]^*$$

where the D^J denotes the usual rotation function and $\lambda = \lambda_1 - \lambda_2$. The spherical angles (θ, ϕ) describe the orientation of the decay axis in the rest frame. The helicity decay amplitudes F^J have the relationships, from parity conservation,

$$F^J_{\lambda_1 \lambda_2} = \eta\,(-1)^J \;\; F^J_{-\lambda_1 - \lambda_2}$$

and, from the fact that the decay particles are identical,

$$F^J_{\lambda_1 \lambda_2} = (-1)^J \;\; F^J_{\lambda_2 \lambda_1}$$

Note that, if $J = 1$, $F^J = 0$ if $\lambda_1 = +1$ and $\lambda_2 = -1$ since this would violate conservation of the z-component of spin along the decay axis. If the spin-1 decay particles are massless, then the zero helicities are not allowed. It is now easy to show that the allowed quantum numbers are

$$J^{PC} = 0^{\pm +}, 2^{\pm +}, 3^{++}, 4^{\pm +}, 5^{++}, ...$$

The symmetry relationships given above for the helicity amplitudes apply equally well when the decay particles have spin zero; one finds immediately that in this case one must have J and η even.

The initial state of the double-pomeron production is in reality a flavorless and colorless gluonic bundle. It follows therefore that the final state should be rich in gluonic excitations, i.e. glueballs and hybrids. In contrast, two offshell photons couple preferentially to charged quarks, e.g. $u\bar{u}$ or $c\bar{c}$ if the energy is high enough, leading to the production of quarkonia and multiquark states.

2. B Physics at RHIC

One of the more fundamental questions confronting the Standard Model based on the group $SU(3) \otimes SU(2) \otimes U(1)$ is the problem of understanding the origin of the CP violation and of the existence of three generations of quarks and leptons. In a conventional parameterization of the Standard Model, the CP violation arises from a single non-zero phase in the Cabbibo-Maskawa-Kobayasi (CKM) matrix. The study of the CP violation therefore involves, among others, precision measurements of all the elements of the CKM matrix.

It is now an accepted norm that, in addition to the $K^0\bar{K}^0$ system, the CP-violation effects should occur substantially in the B decays. There is therefore a tremendous push to start B physics at LEP and TEVATRON. In addition, asymmetric e^+e^- machines as B factories have been proposed at SLAC[12], KEK[13], Cornell[14] and CERN[15]. A proposal also exists to build a dedicated detector[16] for B physics at the SSC.

With several crucial additions and modifications to the QGS, one can contemplate carrying out B physics at RHIC. A possibility of B physics at RHIC has been previously investigated by N. Lockyer et al.[17]. In terms of certain key parameters, the QGS described above is essentially similar to the detector studied by them.

Of particular interest are the self-tagging B decays: $B_d^0 \rightarrow K^+\pi^-$ and $\bar{B}_d^0 \rightarrow K^-\pi^+$. The P_t of the B mesons at RHIC are typically about 4.4 GeV/c. About 90% of the decay tracks are contained within ± 2 units of pseudo-rapidity, and the p_t of the $K^\pm$ ranges from 0.7 GeV/c to 7.0 GeV/c, in contrast to the typical 300-MeV/c track for the underlying events. As $c\tau = 350$ μm for the B mesons, it is necessary to measure vertices at an accuracy of 10 μm in order to be efficient in picking out B events from the background.

These considerations argue for a micro-vertex detector, e.g. the silicon drift chamber[18] with a position resolution in both x and y directions at 10 μm. It is envisioned that a three-layer barrel vertex detector will be fully instrumented for triggers, with a fast on-line processor called on to determine in real time the production and decay vertices. A B-trigger may be that in which a decay vertex is separated by more than 30 μm from the production vertex. More details are given in the next section.

At the highest luminosity for $p \times p$ at RHIC, there may be one to two interactions per bunch crossing, with the time separation between bunches expected to be 225 ns. The drift-chamber module, described in the next section, has an average drift space of 5 mm and the maximum drift time of 50 to 100 ns depending on the type of gas mixture used. As the interaction diamond length is ± 22 cm, multiple events from on a single bunch crossing can be resolved offline in principle as distinct clusters separated along the beam line.

The RHIC machine may operate in a $p \times p$ mode with a luminosity of 10^{32} cm^{-2} sec^{-1} at 250 $\times$ 250 GeV. The estimated $B\bar{B}$ cross section at these energies is about 10 μb, and a run of 10^7 sec would produce roughly 10^{10} $B\bar{B}$ pairs. Assume that the fraction of $B_d^0\bar{B}_d^0$ pair production is 20% of that of the B as a whole; that the branching ratio for $B_d^0 \to K^+\pi^-$ is 10^{-5}; that the overall trigger and other efficiencies add up to 1%. Then from a sample of $10^{10} B\bar{B}$ events, a CP asymmetry of 20% could be observed at the level of 3σ effect.

This exercise shows that the B physics at RHIC can be competitive with other machines. Other B decay modes such as $B_d^0 \to J/\psi K_S$ may not be as competitive.

3. Central Detector at RHIC

The central detector consists of a neutral and charged particle detection device with a 4π coverage, all housed in a moderate-size solenoid magnet with an inner radius of 206 cm and 590 cm long outside. The magnet uses Al coils inside the yoke producing a field strength of 0.5 T. It is designed to identify up to a dozen particles with momenta in the range 0.05–2.50 GeV/c, for a study of meson systems with mass 1.0–3.0 GeV. The central detector is thus given the name QGS, for Quark-Gluon Spectrometer (see Fig. 3).

The QGS consists of a micro-vertex detector (MVD) located within a beam pipe, a drift-chamber module (CDC) surrounding the beam pipe, followed by two ring-imaging Cerenkov counters (RICH1 and RICH2), a time-of-flight (TOF) hodoscope and a lead-scintillation sandwich EM calorimeter, all within the magnet coil. Each end of the magnet is instrumented with a hadron calorimeter. These items are described briefly below.

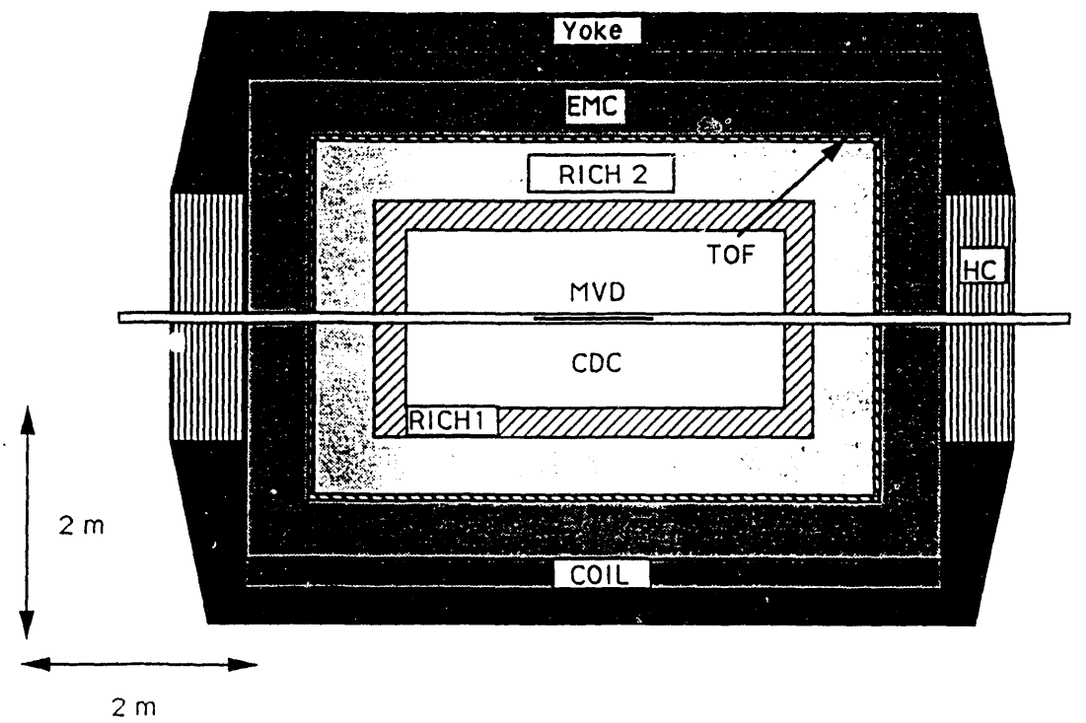

Figure 3: The Central detector: Quark-Gluon Spectrometer (QGS). The major components consist of a micro-vertex detector (MVD), a central drift-chamber module (CDC), two ring-imaging Cerenkov counters (RICH1 and RICH2), a time-of-flight hodoscope (TOF), an electromagnetic calorimeter (EMC), and a hadron calorimeter (HC).

The micro-vertex detector (MVD), shown in detail in Fig. 4, is envisioned to be a silicon drift chamber[18] with its position resolution of 10 μm in both x and y directions. The MVD is a three-layer barrel vertex detector, divided into four quadrants and fully instrumented for triggers. A fast on-line processor finds in real time the production and decay vertices in the $r - z$ plane, where the z axis is along the beam line. An obvious advantage is that tracks are, to first order, linear in this plane, making the pattern recognition easier. Offline analysis will involve finding tracks in the $r - \phi$ plane as well. A possible B trigger is that

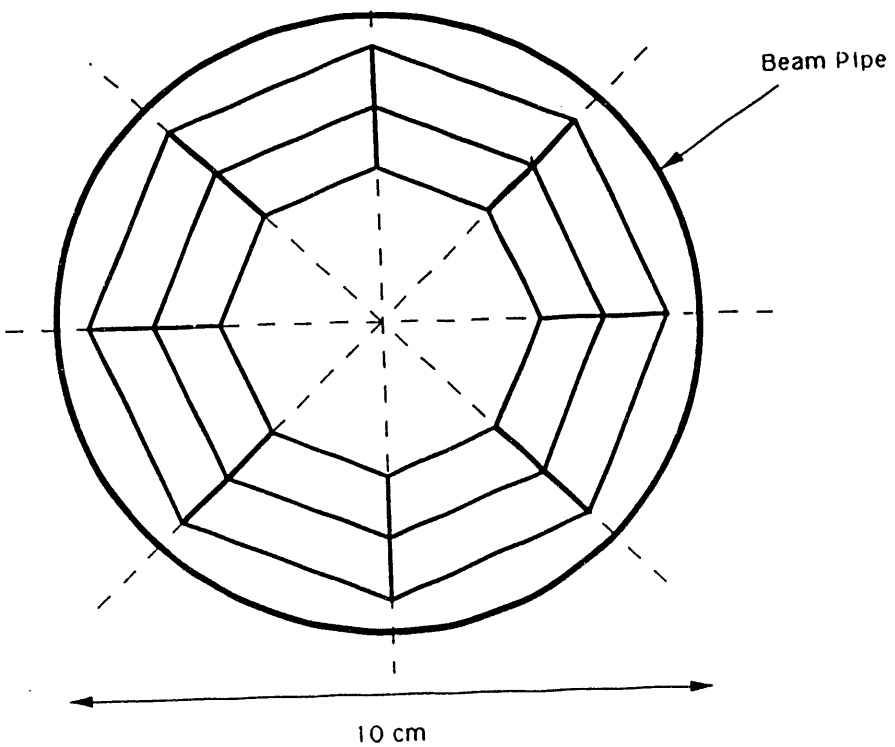

Figure 4: The micro-vertex detector (MVD) inside the beam pipe. It is in the shape of an octagon with four sections, which can be retracted.

in which the decay vertex is separated by more than 30 μm from the production vertex. This requires a very fast on-line computer or a dedicated micro-processor.

The beam-spot size for protons at 250 GeV/c can be approximated by Gaussian with $\sigma = 0.6$ mm. Therefore, the vertex detector can be put as close as 5 mm from the beam center, when the RHIC is in a stable DC mode and the synchrotron radiation is properly shielded. However, for the time being, a more conservative design is adopted; the innermost layer of the MVD has an average radius of 2.4 cm, and the second and third layer at radii of 3.3 and 4.2 cm, respectively. The beam-pipe diameter for the QGS will be fixed at 10 cm.

The drift-chamber module is 3.2 m long along the beam; it starts at a radius of 6 cm and extends to 76 cm. The size of drift cells (5 mm) is dictated by the time interval of 225ns between bunch crossings. The whole module is divided into 9 layers, each containing two axial sense wires and two stereo wires at angles from 40 mr to 80 mr. In all there will be some 9100 sense wires. The rms error on the transverse momentum is estimated to be

$$\frac{\delta p_\perp}{p_\perp} = 1.5\%\ p_\perp(\ \mathrm{GeV/c})$$

assuming a measurement accuracy of 200 μm and a field of 0.5 T. The angular resolution is, from multiple scattering,

$$\delta\theta = \frac{1.3\ \mathrm{mr}}{p_\perp(\ \mathrm{GeV/c})}$$

Particle identification is provided by the dE/dx measurement. Assuming an average of 36 measurements per track, the resolution is expected to be 15% FWHM. This provides a 3σ π/K separation up to about 0.6 GeV/c.

At the highest luminosity for $p \times p$ at RHIC, there may be one to two interactions per bunch crossing, with the time separation between bunches expected to be 225 ns. The drift-chamber module has an average drift space of 5 mm and the maximum drift time of 50 to 100 ns depending on the type of gas mixture used. As the interaction diamond length is ± 22 cm, multiple events from on a single bunch crossing can be resolved offline in principle as distinct clusters separated along the beam line. However, one may, for an extra margin of safety, decrease the drift space to 2.5 mm, increasing the total number of sense wires to 18200, and in addition use a gas mixture with a fast drift velocity of 100 μm/ns, thus reducing the maximum drift time to 25 ns.

In order to distinguish the mass of the B_d^0 from that of the B_s^0, a momentum resolution of the drift-chamber module better than that given above may be necessary; one may then have to replace the conventional solenoid magnet with a superconducting one and increase the field strength from 0.5 T to 2.0 T, for a factor of four gain in the momentum resolution.

The RICH1 and RICH2 detectors envisaged here are patterned closely after the DELPHI design[19]. Several relevant formulae are first introduced here for convenience. Let n be the index of refraction of a radiating medium, and let β be the velocity of a particle in

the medium. Then, the threshold velocity or its $\eta = \beta\gamma$ and the Cerenkov angle are given by

$$\eta_t = \frac{1}{\sqrt{n^2-1}} = \frac{1}{\sqrt{2\delta+\delta^2}}$$

$$\tan\theta_c = \sqrt{(n\beta)^2-1} = \beta\sqrt{\frac{1}{\eta_t^2}-\frac{1}{\eta^2}}$$

where $\delta = n-1$. Let L be the length of the radiator plus the drift space. Then, the radius of the Cerenkov ring is

$$r = L\tan\theta_c = L\sqrt{(n\beta)^2-1}$$

Or, expressing in terms of η_t, one obtains

$$r = \left(\frac{L}{\eta_t}\right)\beta\sqrt{1-\left(\frac{\eta_t}{\eta}\right)^2}$$

which shows that the maximum r is given by L/η_t for $p = \infty$. RICH1 extends from a radius of 76 cm to 101 cm and is 370 cm long on the outside. The front segment consists of a 1cm-thick liquid Freon (C_6F_{14}) with an index of refraction $n = 1.277$ ($\eta_t = 1.26$), so that a relativistic particle produces Cerenkov light of 11.1 cm radius at the end of a 13 cm drift region ($L = 14$ cm). The threshold momenta are 0.18 and 0.62 GeV/c for π and K, respectively. It is then followed by a 4.4cm-thick photon-conversion region containing $CH_4(75\%)+C_2H_6(25\%)$ and TMAE (Tetrakis Dimethyl Amino Ethylene). The readout is accomplished by a multi-wire proportional chamber with 1.5 mm wire spacing. The drift time is about 25 μs, which implies that this RICH1 counter is not a trigger device. The offline π/K separation is impressive, starting at 0.18 GeV/c and extending to 3.0 GeV/c. The upper limit is determined by the difference in radii of the π and the K rings, 11.1 and 10.7 cm, respectively at $p = 3.0$ GeV/c, and the experimental resolution of the rings as given by the wire spacing.

As the $K^{\pm}$ momenta range up to 10.0 GeV/c and above for B decays, a second counter RICH2 will be added to handle momenta between 3.0 to 10.0 GeV/c. It extends from a radius of 101 cm to 151 cm and is 470 cm long outside. Following the DELPHI design, the Cerenkov light is reflected back via parabolic mirrors to the proportional chamber, to be read out. The radiating medium is C_4H_{10} (isobutane) at atmospheric pressure and room temperature with $\eta_t = 19.8$. Assuming a nominal L value of 100 cm, the maximum r is

seen to be 5.05 cm. For momenta between 2.8 and 9.8 GeV/c, the RICH2 detector works as a threshold counter. Above 9.8 to 25 GeV/c the detector can separate a K from a π; their Cerenkov rings at $p = 25$ GeV/c have radii of 5.0 and 4.6 cm, respectively.

The TOF system is located at a radius of 151 cm and is 470 cm long. It consists of 190 5x5 cm scintillation counters, each viewed by two photomultipliers. The π/K time separation for a path length L is

$$\Delta t(\text{ ps}) = \left(\frac{100}{3}\right) L(\text{ cm}) \left(\frac{E_K}{p} - \frac{E_\pi}{p}\right)$$

The resolution is conservatively estimated to be 250 ps, providing a 3σ π/K separation from 0.08 GeV/c to 0.6 GeV/c. Thus it can be used as an independent check of both the drift-chamber module and the RICH counters. It can also be used as a component in the charged particle triggers.

The EM calorimeter covers radii from 156 cm to 206 cm and is 580 cm long outside. In order to achieve good efficiency for soft photons, the detector is placed inside the magnet coil. It consists of 4700 10x10 cm towers, each with 84 layers of 6 mm lead-scintillation sandwiches (1 mm of lead and 5 mm of plastic scintillator) for a total of $15X_0$ and viewed by a photodiode through a wave-length shifter. The endcap EM calorimeters are similar in design, consisting of 1530 10x10 cm towers. A similar device[20] was used by ARGUS. The energy resolution is expected to be

$$\frac{\delta E}{E} = \frac{7\%}{\sqrt{E(\text{ GeV})}}$$

for photon energies from 0.07 GeV to 3.0 GeV.

The end caps of the magnet have cutouts with radius 100 cm, and two hadron calorimeters with the active areas at radii from 5 cm to 100 cm will be installed in this space. Each calorimeter consists of 30 iron-scintillation disk-shape sandwiches. Both the iron plate and the plastic scintillator are 1 cm thick, and the periphery of the scintillator is edged with a wave-length shifter, which is read out by a photomultiplier. It is estimated that the energy resolution is

$$\frac{\delta E}{E} = \frac{60\%}{\sqrt{E(\text{ GeV})}}$$

so that a 10 GeV/c particle can be measured with an accuracy of about 20%. For the $Au \times Au$ run, the two hadron calorimeters will be used to veto on any particle with energy greater than 10 GeV/c. It is expected that about 90% of all the diffractive dissociation events can thus be eliminated at the trigger level.

4. Triggers at RHIC

The trigger for **PP** interactions relies on a set of four scintillation counters within the Roman pots. For $p \times p$ runs, two triggers are possible with the Roman pots, 'up-up' and 'down-down.' This means that both of the counters above (below) the beam line at either side of the intersection region are triggered for 'up-up' ('down-down'). The triggers will be augmented with signals from the QGS, utilizing among others the hits in the EM calorimeter. Each hit above the minimum energy threshold, but below the maximum allowed energy, e.g. 10 GeV, is treated with equal weight; a fast microprocessor sums up independently the x, y and z projections of the location of the hit with respect to the midpoint of the intersection region. The trigger requires that the three sums are within a small preset range. This algorithm ensures that an event with a large missing energy in any direction will be eliminated, on the average. Note also that this technique treats charged and neutral particles on an equal footing.

For $Au \times Au$ runs, instead of the Roman pots, the trigger relies primarily on signals from the QGS to pick out two-photon events, accompanied by vetos at two end-cap hadron calorimeters and the four lead-scintillation barrel counters located 10 m and 40 m away from the intersection region. The vetoes guard against the small-angle beam deflections and the diffractive dissociation of the beams.

A Monte Carlo study is planned to assess the efficacy of the x-, y- and z-projection methods described above in selecting production of low-mass hadrons in the central region.

The key to a successful study of the B decays, $B_d^0 \to K^+\pi^-$ and $\bar{B}_d^0 \to K^-\pi^+$, at RHIC lies in detecting a decay vertex, a V, separated from the production vertex at the trigger level. Given $c\tau = 350$ μm for the B and a typical B momentum around 5 GeV/c, it is desirable to be able to detect a V separated by 50 μm or less from the production vertex. A fast online computer or a dedicated micro-processor will be used to find in the

$r-z$ plane the production vertex first, and then a V separated from the production vertex by at least 30 μm. It is possible that the same algorithm can be applied to the $r-\phi$ plane as well, for detection at trigger level of a clean V. One may also rely on detection of a charged K for a higher level trigger; however, a more careful Mote Carlo study will be needed for this and other possible trigger schemes.

5. Conclusions

In this note a brief description is given of an exciting opportunity to carry out hadron spectroscopy experiments at RHIC. The machine is slated to be ready for physics in 1997. As such, it provides timely opportunities for further investigation into the outstanding problems in hadron physics, in particular those that cannot easily be tackled with the machines currently available in the world.

The key idea for RHIC is that by concentrating on the extreme double-peripheral region, the machine is used to produce hadronic systems at low $\sqrt{s}$ in the range 1.0–10.0 GeV.

The sub-processes responsible for the hadronic system in the central region may be expressed either as pomeron + pomeron $\rightarrow$ hadrons or as $\gamma^* + \gamma^* \rightarrow$ hadrons. The double-pomeron interactions are expected to produce glueballs and hybrids preferentially, while the two-offshell-photon initial states should couple predominantly to quarkonia and multiquark states. A whole gamut of J^{PC}-exotic mesons ($0^{+-}, 0^{--}, 1^{-+}, 2^{+-}$, $3^{-+}, 4^{+-}$,..) may be seen either directly in both types of interactions or in association with a single recoil photon in the final state. Another important distinction is that the hadronic system from a double-pomeron interaction has zero net flavor, whereas an $I^G = 1^-$ meson can couple readily to a two-photon initial state. The salient feature of this proposal lies in the fact that, for the first time, a study of the pomeron-pomeron interactions can be mounted with the same experimental setup as that of the photon-photon interactions.

In addition, the QGS with a micro-vertex detector and two RICH counters can tackle the CP-violation effects in the B decays. The key element in this effort would have to be the capability to trigger on the B-decay vertices separated by more than 30 μm from the

production vertex. The upgraded QGS may also serve as the apparatus for a study of χ_c and χ_b states.

Acknowledgements

The authors are indebted to P. Rehak, S. Protopopescu and F. Paige for several helpful discussions.

References

1. Conceptual Design of the Relativistic Heavy Ion Collider (RHIC), BNL, Upton, NY (May 1989), BNL-52195.
2. S. U. Chung, W. Kern and H. J. Willutzki, 'Hadron Spectroscopy at RHIC,' Proc. Fourth Workshop on Experiments and Detectors at RHIC, BNL, July 1990, BNL-52262 (1990), p. 207.
3. T. Akesson et al., Phys. Lett. 133B, 268 (1983);
   T. Akesson et al., Nucl. Phys. B264, 154 (1986);
   P. C. Cecil, Ph. D. Thesis, Cavendish Laboratory, Cambridge, England, Rutherford preprint RAL -T -004 (1984).
4. K. L. Au, D. Morgan and M. R. Pennington, preprint RAL -86 -076 (1986), Phys. Rev. D35, 1633 (1987).
5. D. Bernstein et al., NIM Vol. 226, 301 (1984).
6. K. Goulianos, 'Diffractive interactions of hadrons at high energies,' Physics Reports, Vol. 101, No. 3 (1983).
7. S. U. Chung, 'Kinematics, Phase Space and Phenomenological Amplitudes for Double-Pomeron Exchange Reactions,' BNL Internal Report OG-734 (1983).
8. A. Skuja and D. H. White, 'Two-Photon Physics at RHIC,' RHIC Workshop, BNL-51921 (1985), p. 289.
9. S. U. Chung, D. P. Weygand and H. J. Willutzki, 'Double-Pomeron and Two-Photon Processes at RHIC,' BNL-QGS-02-91.
10. M. Jacob and G. C. Wick, Annals of Physics Vol. 7, 404 (1959).
11. S. U. Chung, 'Spin Formalisms,' CERN Yellow Report, CERN 71-8 (1971).
12. The Physics Program of High-luminosity Asymmetric B Factory at SLAC, SLAC-353 (October 1989).

13. H. Aihara, B Factory at KEK, Proceedings of the U.C.L.A. Workshop on Linear Collider $B\bar{B}$ Factory–Conceptual Design (January 1987), edited by D. Stork.

14. The Workshop towards establishing a b Factory, Syracuse Univ., Syracuse, NY (September 1989), edited by M. Goldberg and S. Stone.

15. Feasibilty Study for a B-meson Factory in the CERN ISR Tunnel, T. Nakada (Editor), CERN 90-02.

16. Expression of Interest for a Bottom Collider Detector at the SSC (May 1990), N. Lockyer (Spokesperson, Univ. of Pennsylvania).

17. Lockyer, et al., Proceedings of the Third Workshop on Experiments and Detectors for RHIC (July 1990), p. 157.

18. P. Rehak et al., NIM Vol. A248, 367 (1986).

19. R. Arnold, et al., NIM Vol. 270, 255 (1988); NIM Vol. 270, 289 (1988).

20. W. Hofmann et al., NIM Vol. 163, 77 (1979).

END

DATE
FILMED
2/07/92

I